Catal Lett (2015) 145:985–994
DOI 10.1007/s10562-014-1394-2

PERSPECTIVE

The Nature of Surface CrO_x Sites on SiO_2 in Different Environments

Anisha Chakrabarti · Israel E. Wachs

Received: 22 August 2014 / Accepted: 6 October 2014 / Published online: 17 October 2014

Abstract This perspective article critically reviews the catalysis literature on the nature of the surface CrO_x sites present on SiO_2 in different environments. The recent application of in situ spectroscopic techniques that directly monitor the surface chromia sites on silica in different environments has significantly improved our fundamental understanding of supported CrO_x/SiO_2 catalysts.

Keywords Spectroscopy · UV–Vis · Polymerization · Chromia · Raman · H_2-TPR

1 Introduction

In the early 1950s, J. P. Hogan and R. L. Banks of Phillips Petroleum Company made the discovery that ethylene can be converted to polyethylene by a chromium oxide–silica–alumina catalyst [1] that was subsequently commercialized. The Phillips type catalyst system, CrO_x supported on an amorphous support, such as silica, is one of three types of catalysts currently used for olefin polymerization. The other two types are Ziegler–Natta and single-site homogeneous catalysts or supported homogeneous catalysts, both of which require an activator. The appeal of the Phillips catalyst lies in its many advantages: (i) yielding over 50 different types of polyethylene, (ii) functioning without activators, and (iii) operating at low temperatures and pressures [1–3]. The original catalyst system has since been fine-tuned and ethylene polymerization by silica supported CrO_x catalysts is now responsible for ~40–50 % of all high-density polyethylene (HDPE) produced [3]. In spite of the extensive research studies that have been performed about the supported CrO_x/SiO_2 catalyst system over the past six decades, the same fundamental structural and mechanistic questions are still being debated [1–4]. For example, the initial molecular structure of the oxidized surface $Cr^{+6}O_x$ site has been proposed to be present as isolated surface dioxo CrO_4, isolated surface mono-oxo CrO_5, and dimeric surface Cr_2O_7, while the chromia oxidation state during ethylene polymerization has been proposed to be reduced Cr^{+2} and Cr^{+3}. This perspective focuses on the nature of the surface chromia sites on silica in the different environments [oxidizing (hydrated and dehydrated) and reducing (CO, H_2 and C_2H_4)] to stress what is currently known and what more needs to be done to fully understand the nature of the surface CrO_x sites present for the silica-supported chromium oxide catalysts.

2 Advantages and Disadvantages of Characterization Techniques for Supported CrO_x/SiO_2 Catalysts

Many characterization techniques have been used to investigate supported CrO_x/SiO_2 catalysts, but each method has its advantages and disadvantages. The typical techniques have been ultraviolet–visible diffuse reflectance spectroscopy (UV–Vis DRS), electron paramagnetic resonance (EPR) spectroscopy, infrared (IR) spectroscopy, Raman spectroscopy, X-ray absorption spectroscopy (XAS), and temperature programmed surface reaction (TPSR) spectroscopy.

UV–Vis spectroscopy probes electronic transitions, allowing for determination of the coordination and

A. Chakrabarti · I. E. Wachs (✉)
Operando Molecular Spectroscopy and Catalysis Laboratory,
Department of Chemical Engineering, Lehigh University,
Bethlehem, PA 18015, USA
e-mail: iew0@lehigh.edu

oxidation state of charge transfer (CT) Cr^{+6} bands and d–d $Cr^{+5,+3}$ transition bands. The broad UV–Vis bands, however, make it difficult to distinguish between multiple species and the d–d transitions are weak and may overlap nearby CT or d–d bands. The UV–Vis edge energy, Eg, provides direct information about the extent of oligomerization of the surface CrO^{+6} sites (monomer, dimer, etc.).

EPR spectroscopy can detect paramagnetic (containing unpaired electrons) Cr^{+5} and Cr^{+3} sites and provide their coordination information. Although Cr^{+2} sites are also paramagnetic, its EPR signal is too weak to be detected with conventional EPR spectrometers.

IR spectroscopy is a very powerful technique that provides molecular vibrational information and is more sensitive to asymmetric vibrations due to its selection rules. IR has been valuable in determining the anchoring sites of the surface CrO_x species since the Si–OH vibrations are rather intense. The strong IR absorption by the SiO_2 support, however, only allows the monitoring of Cr–O vibrations in the ~850–970 cm^{-1} window. IR spectroscopy also provides vibrational information about surface intermediates and reaction products formed on the catalyst surface.

Raman spectroscopy also probes molecular vibrations and is complementary to IR but is more sensitive to symmetric vibrations. The weak Raman bands from the SiO_2 support allows monitoring vibrations of surface CrO_x sites from 0 to 4000 cm^{-1} for the supported CrO_x/SiO_2 catalyst system.

XAS includes X-ray absorption near edge structure (XANES) and extended X-ray absorption fine structure (EXAFS). XANES allows determination of oxidation and coordination states by observing the pre-edge energy and selection rules. The position of the pre-edge energy reflects the oxidation state. For CrO_4 coordinated sites, there is a strong pre-edge, but the pre-edge is forbidden for CrO_6 coordinated sites with inverse symmetry due to the XANES selection rules. EXAFS allows determination of Cr–O bond distances. The shortcoming of XAS is that it averages over multiple sites if a single site is not present, which complicates analysis since the concentration of sites may not be known. Furthermore, the XAS signal reflects the dominant species if two sites are present with one having a high concentration and the other being a minority species (e.g., CrO_x and Cr_2O_3 or Cr^{+6} and Cr^{+3}). Thus, it is critical to make sure that Cr_2O_3 nanoparticles are not present since they will complicate analysis of the surface CrO_x species. The presence of multiple Cr oxidation states also complicates the analysis.

Temperature Programmed Surface Reaction (TPSR) spectroscopy chemically probes the reactivity of the supported chromia phase on silica. During TPSR, the catalyst temperature is ramped in the presence of a chemical reactant and the gaseous reaction products are continuously monitored with an online mass spectrometer. TPSR has the capability to discriminate between multiple surface CrO_x sites on silica, quantify their relative concentrations and determine their reaction kinetics.

No single characterization technique is sufficient to fully characterize the supported CrO_x sites on SiO_2 given the limitation of each characterization method. Applications of multiple characterization techniques, however, can tease out the desired fundamental information. Consequently, as will be seen below, the most informative studies employ multiple characterization techniques to yield a comprehensive model of the supported CrO_x/SiO_2 catalyst system.

3 Hydrated Supported CrO_x/SiO_2 in Initial Oxidized Catalyst under Ambient Conditions

The supported CrO_x on silica catalyst system is prepared by the incipient-wetness impregnation method employing a chromia precursor that is soluble in the solvent being employed. The impregnated catalyst is initially dried overnight at room temperature in air, further dried in air at ~100 °C and then calcined at elevated temperatures (~400–800 °C) in an oxidizing environment [3]. Upon exposure to ambient air, the oxidized catalyst becomes hydrated by adsorption of moisture, which affects the molecular structures of the oxidized surface CrO_x species on SiO_2 [5, 6].

The lack of appreciation that the surface CrO_x sites on silica are hydrated under ambient conditions and limited application of characterization techniques capable of discriminating between multiple chromia states has also led to much confusion about the nature of the hydrated surface CrO_x sites on silica. Raman spectroscopy, however, readily discriminates between different chromia molecular structures since each molecular structure gives rise to a unique vibrational spectrum [7]. The first application of Raman spectroscopy to the examination of hydrated supported CrO_x/SiO_2 catalysts was reported by Hardcastle and Wachs [5]. The hydrated surface CrO_x phase on silica was found to consist of monomers (CrO_4), dimers (Cr_2O_7), trimers (Cr_3O_{10}) and tetramers (Cr_4O_{13}), with the extent of oligomerization increasing with chromia loading. The oligomerization of the surface CrO_x sites on SiO_2 with increasing chromia loading is a consequence of the decreasing pH at point of zero charge (PZC) of the thin aqueous film present on the supported CrO_x/SiO_2 catalyst [8].

Weckhuysen et al. [9] investigated supported chromia catalysts on silica under ambient conditions as a function of Cr loading (0.2–8 % Cr) [9]. The UV–Vis DRS spectra for the lowest Cr loading exhibited two bands dominating at 348 and 240 nm with a shoulder at 429 nm, and the corresponding Raman spectra contained just one band at

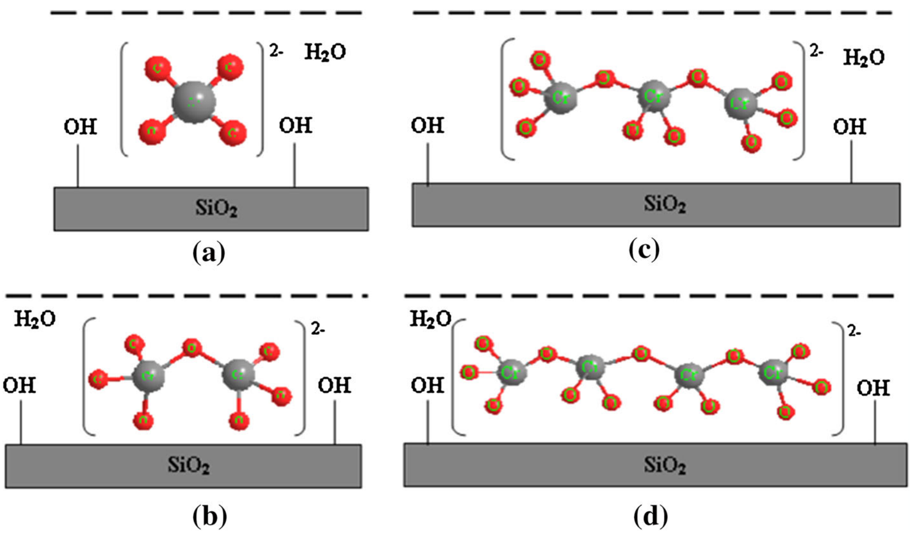

Fig. 1 Schematic of molecular structures of "hydrated" CrO_x sites on the SiO_2 support: (a) monomer CrO_4^{2-}, (b) dimer $Cr_2O_7^{2-}$, (c) trimer $Cr_3O_{10}^{2-}$, and (d) tetramer $Cr_4O_{13}^{2-}$

895 cm^{-1}. These spectral features indicate hydrated surface dichromate species [7, 10]. As the Cr loading was further increased, the UV–Vis bands broadened and shifted from 348 to 370 nm, and the shoulder at 429 nm became more pronounced. With increasing Cr loading, the Raman spectra contained bands at 380, 850, 900 and 960 cm^{-1} that are representative of hydrated trichromate and tetrachromate species [7]. The XANES spectra of the hydrated catalyst exhibited a sharp pre-edge at about 5992 eV, which is a dipole-forbidden transition 1s → 3d characteristic of 3d metal oxides not possessing an inversion center such as tetrahedral coordinated CrO_4. The corresponding EXAFS spectra of the hydrated catalyst possessed one FT peak at ~1.3 Å with an out-of-phase shift correction. After curve-fitting of the EXAFS spectra, the Cr–O distance and coordination number for the first shell were determined to be 1.58 Å and 3.7, respectively, which are similar to those of the CrO_4 unit in the K_2CrO_4 reference compound ($R = 1.62$ Å and $N = 3.9$). The combination of the spectroscopic techniques allowed for a full picture of the hydrated chromia species on silica. It was determined that the nature of the hydrated surface CrO_x species only depends on the pH at PZC, which leads to dichromates at low Cr loading and trichromates and tetrachromates at high Cr loading. Crystalline Cr_2O_3 nanoparticles also form at higher Cr loading.

The molecular structures of the hydrated surface CrO_x sites on SiO_2 are schematically shown in Fig. 1.

4 Supported CrO_x/SiO_2 in Initial Oxidized Catalyst under Dehydrated Conditions

The hydrated surface CrO_x species on SiO_2 become dehydrated and change their molecular structures upon heating to elevated temperatures [5]. Early thermogravimetric analysis (TGA) by Hogan examined the loss of water by silica upon adsorption of chromia on dehydrated SiO_2 and led to the conclusion that surface CrO_x on silica is mainly present as isolated CrO_4 sites, although at high temperatures dimeric Cr_2O_7 sites cannot be excluded [11]. This conclusion was based on the model that only isolated surface CrO_4 and dimeric Cr_2O_7 sites are present and anchor to the silica support by titrating surface Si–OH hydroxyls. Each chromia structure was assumed to consume two surface Si–OH hydroxyls with a ratio of 2 Si–OH/Cr for the isolated CrO_4 and 1 Si–OH/Cr for the dimeric Cr_2O_7. This model also assumes that the supported chromia phase is (i) 100 % dispersed (crystalline Cr_2O_3 nanoparticles are not present), (ii) only possesses CrO_4 coordination and (iii) the SiO_2 surface is not altered by anchoring of the surface chromia species (e.g., siloxane Si–O–Si bonds do not participate). In spite of the absence of direct spectroscopic evidence about the nature of the surface CrO_x sites on SiO_2, this early publication introduced the concept that the surface CrO_x sites on SiO_2 are only present as isolated CrO_4 and dimeric $O_3Cr–O–CrO_3$ structures [11].

Zecchina et al. were the first group to apply in vacuo IR and UV–Vis spectroscopy to examine the dehydrated supported CrO_x/SiO_2 catalysts [10]. The IR spectra exhibited a broad band at 925 cm^{-1} that was assigned to surface dichromate sites on silica. Recent DFT and Raman analysis, to be presented below, demonstrate that this IR band is actually the vibration from the bridging Cr–O–Si bond and does not provide any information about the structure of dehydrated the surface CrO_x sites on silica. In the silanol stretching region (~3700 cm^{-1}), the intensity of the Si–OH band linearly decreased with increasing chromia loading up to ~5 % Cr and the silanol concentration did not further decrease with increasing Cr loading.

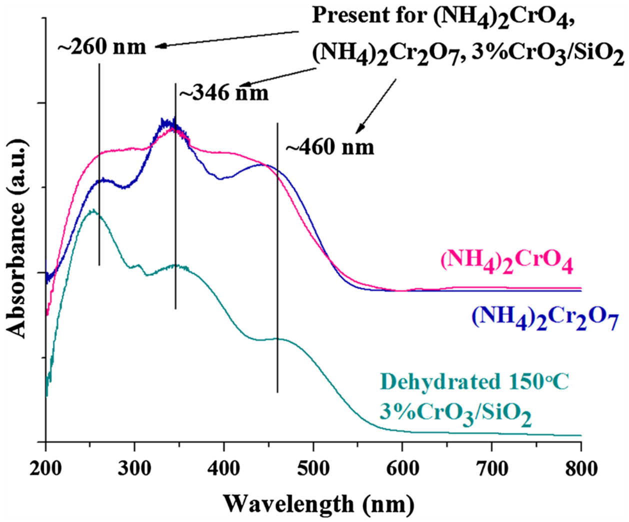

Fig. 2 UV–vis of reference compounds under ambient conditions

The leveling off of the consumption of the surface silanols coincides with the formation of crystalline α-Cr_2O_3 nanoparticles. The ratio of surface Cr to Si–OH consumed was determined to be ~1, which suggested surface dichromate sites since isolated surface chromate sites would be expected to be ~0.5 according to Hogan's model. The UV–Vis spectra contained O → Cr^{+6} ligand-to-metal charge transfer (LMCT) bands below 556 nm that were assigned to surface dichromate and isolated surface chromate sites, with relative intensities suggesting that the surface dichromate dominates. The broad nature of these UV–Vis bands at 256 and 351 nm with the shoulder at 385 nm, however, can be assigned to both isolated surface chromate and surface dichromate since clear distinction between both structures is complicated by their broad and overlapping UV–Vis bands as shown in Fig. 2. The band at 461 nm was assigned to dichromates, but this band is also present for Cr_2O_3 nanoparticles. A small d–d band above 556 at 714 nm was attributed to chromia in an oxidation state lower than Cr^{+6} and was thought to be from surface $Cr^{+5}O_4$ sites on silica. This pioneering characterization study, however, could not clearly provide spectroscopic identification of the nature of the dehydrated surface CrO_x sites on SiO_2 since the UV–Vis bands for the dehydrated supported CrO_x/SiO_2 catalyst and the CrO_4 and Cr_2O_7 reference compounds are too broad to allow assignment as shown in Fig. 2.

Fubini et al. also reported in vacuo UV–Vis–NIR spectra of dehydrated supported CrO_x/SiO_2 catalysts and detected LMCT bands at 476, 345, and 238 nm from surface $Cr^{+6}O_x$ sites. These bands were very close to those observed by Zecchina et al. with the exception of an additional shoulder at ~385 nm. Comparison with K_2CrO_4, containing isolated CrO_4 units, and $K_2Cr_2O_7$, consisting of dimeric Cr_2O_7 units, suggested that surface dichromate sites were the dominant surface chromia sites on silica [12]. This group came to the same conclusions as Zecchina et al.

In the past two decades, there was a growing emphasis on investigations with in situ characterization techniques that provided *direct* observation of the dehydrated surface CrO_x sites on silica.

Weckhuysen et al. examined the structure of the dehydrated surface CrO_x sites on SiO_2 as a function of Cr loading with in vacuo XANES/EXAFS, in situ Raman and in situ UV–Vis spectroscopy [9, 13]. The XANES pre-edge intensity possessed a strong feature at 5992 eV indicative of $Cr^{+6}O_4$ coordination. The corresponding in situ EXAFS spectra contained 2 Cr–O distances at 1.53 Å and 2.05 Å with coordination numbers of 2.2 and 2.1, respectively. An additional Cr–Cr peak was present at ~3.1 Å with a coordination number of ~0.5. Two possible explanations were given. In the first interpretation, polychromate species are present with Cr=O at 1.53 Å and bridging Cr–O–Si at 2.05 Å. Alternatively, the 1.53 Å distance could be related to surface polychromate sites and the 2.05 Å peak is from the presence of Cr^{+3} oxide species. The Cr–Cr peak at ~3.1 Å is also consistent with Cr_2O_3 nanoparticles. Weckhuysen et al. favored the latter interpretation because it was more in line with the corresponding UV–Vis spectra that detected Cr^{+3} [9]. The in situ UV–Vis bands for the supported CrO_x/SiO_2 catalysts gave bands at 645, 455, 328 and 247 nm, with a weak shoulder at 370 nm. These UV–Vis spectra were deconvoluted into 11 bands [13]: 3 weak bands (645, 465, and 295 nm) assigned to $Cr^{+3}O_6$, 4 bands assigned to isolated $Cr^{+6}O_4$ (476, 370, 294, and 268 nm) and 4 bands assigned to dimeric $Cr^{+6}{}_2O_7$ (455, 323, 282, and 246 nm). The intensity ratio of the 370 nm band for isolated CrO_4 and the 323 nm band for dimeric Cr_2O_7 was employed to estimate the ratio of isolated/dimeric surface chromia species, which was found to be ~0.62 for 0.2 % Cr loading. In situ Raman spectra of the dehydrated catalysts, unfortunately, could not be collected with the 514.5 nm laser due to strong sample fluorescence. More recent successful Raman analysis of dehydrated supported CrO_x/SiO_2 catalysts confirmed the presence of Cr_2O_3 nanoparticles at loadings of 4 % Cr and greater [14]. It was concluded that under dehydrated conditions and very high Cr loading on silica, surface polychromates and Cr_2O_3 nanoparticles dominate [9].

The in situ XANES/EXAFS studies by Groppo et al. agree with the earlier findings of Weckhuysen et al. and demonstrated that the XANES spectra of the dehydrated supported CrO_x/SiO_2 catalysts matched with that of bulk CrO_3, consisting of polymeric dioxo CrO_4 units that are compatible with both dioxo isolated CrO_4 and dimeric

Cr_2O_7 structures [15]. Groppo et al.'s earlier UV–Vis spectra of the dehydrated catalyst showed three main components (250, 333, and 463 nm) assigned to O → Cr^{+6} LMCT transitions, which were quite similar to those previously reported by others [15]. Groppo et al. pointed out the limitations of applying UV–Vis to identify surface chromate species because of their very broad and overlapping bands.

Groppo et al. also employed Raman spectroscopy to determine the structure of the surface chromia species [16]. In situ Raman spectroscopy with the 442 nm laser, as opposed to the 514.5 nm laser previously available, allowed for the first time the elimination of sample fluorescence for the supported CrO_x/SiO_2 catalysts. The Raman spectra gave well-resolved bands at 394 (m), 987 (s) and 1014 (m) cm^{-1} with the 394 and 1014 cm^{-1} bands previously not observed due to strong sample fluorescence with lasers using 514 and 532 nm excitation. The band at 987 cm^{-1} was assigned to the ν_s(O=Cr=O) stretching, the band at 394 cm^{-1} to δ(O=Cr=O) bending, and the band at 1014 cm^{-1} to ν_{as}(O=Cr=O) stretching, as suggested by the DFT calculations of Dines et al. [17]. Groppo et al., however, had some concern about the assignment of the 1014 cm^{-1} band because it was stronger than expected and suggested that there may be some heterogeneity of the surface sites. The Raman spectra also showed an absence of chromia bands at 200–300 and 400–700 cm^{-1} indicating the lack of any surface polymeric chromia species at low Cr loadings. Comparison of DFT calculations and Raman spectra revealed that the presence of surface $Cr^{+6}O_x$ could also modify the pure silica vibrations and the IR band at 908 cm^{-1} band previously reported by Zecchina is actually related to a Si–O vibration affected by anchoring of the surface chromate species to the silica support (e.g., bridging Cr–O–Si bonds). The combination of in situ Raman, IR and UV–Vis spectra of the dehydrated supported CrO_x/SiO_2 catalysts at low chromia loadings on silica led Groppo et al. to conclude that surface $Cr^{+6}O_x$ on SiO_2 is anchored as isolated dioxo surface $(O=)_2CrO_2$ species [16].

The more recent in situ UV–Vis and Raman studies by Lee and Wachs finally provided the fundamental insights about the molecular structures of the dehydrated surface CrO_x sites on SiO_2 [14, 18]. The in situ UV–vis absorption bands at ~250, 340 and 460 nm reflect the presence of $Cr^{+6}O_x$ species on silica [14]. The exclusive presence of isolated surface CrO_x species on silica was demonstrated by the high UV–Vis edge energy (Eg) value that is consistent with isolated CrO_x reference compounds [14]. The corresponding Raman spectrum, with 442 nm laser excitation, exhibited bands at 987 (s) and 1014 (m) cm^{-1}, and the selective reduction of the 987 cm^{-1} band by H_2 showed that both bands originate from two distinct surface CrO_x sites on silica [14]. Corresponding isotopic ^{18}O-^{16}O exchange studies of the surface CrO_x species on silica exhibited splitting of the 987 cm^{-1} band into three bands ($^{16}O=Cr=^{16}O$, $^{16}O=Cr=^{18}O$ and $^{18}O=Cr=^{18}O$) consistent with the dioxo nature of the 987 cm^{-1} band ($(O=)_2CrO_2$). The band at 1014 cm^{-1} was assigned to mono-oxo $O=CrO_4$ sites by comparison with chromium oxide reference compounds, but also contains a small contribution from the ν_{as}(O=Cr=O) stretch of the isolated surface dioxo $(O=)_2CrO_2$ species [18]. These molecular assignments to isolated surface dioxo $(O=)_2CrO_2$ and isolated mono-oxo $O=CrO_4$ sites on SiO_2 were further supported by rigorous DFT calculations that also predicted the greater stability of the dioxo CrO_4 species over the mono-oxo CrO_5 surface species on SiO_2 [19]. This suggests that the surface dioxo CrO_4 species should have a higher concentration than the surface mono-oxo CrO_5 species on the silica support (as will be experimentally shown below with H_2-TPSR). The confusion surrounding the dehydrated molecular structures of surface CrO_x sites on SiO_2 required the application of multiple in situ spectroscopic approaches and techniques (Raman, H_2 reduction, isotopic ^{18}O-^{16}O exchange, XAS, IR, UV–Vis and DFT calculations) for its final resolution. The molecular structures of the two dehydrated surface CrO_x sites on SiO_2 are depicted in Fig. 3.

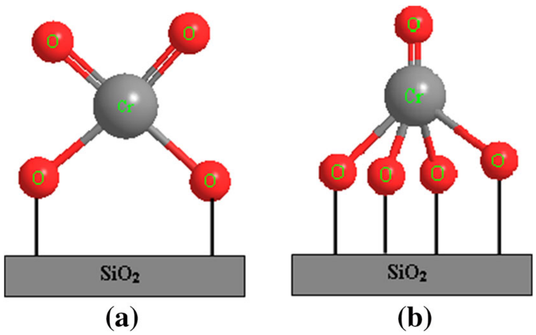

Fig. 3 Schematic of molecular structures of "dehydrated" isolated surface CrO_x sites on SiO_2 support (a) dioxo and (b) mono-oxo

5 Activated Supported CrO_x/SiO_2 Catalysts in Reducing Environments

In industrial ethylene polymerization processes, the supported CrO_x/SiO_2 catalysts are activated with the ethylene reactant [2]. This results in an induction period during which the surface CrO_x catalytic sites are activated by partial reduction to a suboxide for ethylene polymerization. Hogan found during his early studies that reduction in CO could basically eliminate the induction period observed with ethylene, after which activity was immediately observed. It became customary in academic studies to initially activate the supported CrO_x/SiO_2 catalyst by

Table 1 Summary of CO–Activation Studies

Group	Year	Methods	Conclusions
Przhevalskaya et al. [21]	1975	In vacuo EPR, UV–Vis	CO reduction shows Cr^{+2}
Zecchina et al. [22]	1975	In vacuo IR (CO), UV–Vis	2 types of Cr^{+2} 1 type of Cr^{+3}
Fubini et al. [12]	1980	In vacuo UV–Vis	Up to 4 types Cr^{+2} (2 active, 2 inactive)
Rebenstorf et al. [23–25]	~1981–1991	In vacuo IR (CO)	3 dinuclear Cr^{+2} (possibly 4) 2 dinuclear Cr^{+3} (only Cr^{+2} is said to be active)
Gaspar et al. [26]	2001	In vacuo IR (CO)	3 types of Cr^{+2}
Weckhuysen et al. [9, 13]	1995	In situ UV–Vis, XANES/EXAFS, CO-TPR	Cr^{+2} and Cr^{+3}; Cr^{+2}:Cr^{+3} ratio increases with decreasing Cr loading
Groppo et al. [15, 16]	2005	In situ Raman, IR (CO), UV–Vis, XANES/EXAFS	Cr^{+2}

reduction with CO and occasionally H_2. Additionally, pretreating with CO or H_2 affects the polyethylene (PE) yields. Pretreatment with CO modestly increases the PE yield while pretreatment with H_2 can significantly suppress the PE yield and the difference may be related to the presence of moisture produced with the latter [20]. The application of different reducing agents in the literature has caused some confusion since the final activated state may depend on the specific reducing agent being employed.

5.1 Activation of CrO_x/SiO_2 Catalysts with CO

Reduction with CO is a preferred activation method by academic researchers since it does not generate water as a reaction product that may coordinate with the surface CrO_x sites and the findings from different groups are listed in Table 1. Early studies employed CO-TPR to determine how much oxygen was removed from the supported CrO_x/SiO_2 catalysts and found that ~2.05–2.15 O/Cr were consumed indicating that the average oxidation state was Cr^{+2} [9, 13]. This was in agreement with EPR spectra that showed no Cr signal since Cr^{+2} is EPR silent, although it is d4 and paramagnetic in most chemical environments [21]. Chemical probing of the reduced surface sites with CO-IR studies suggested that two surface Cr^{+2} and one surface Cr^{+3} site may be present after CO reduction [22]. Other studies concluded that even more reduced surface Cr sites may be present [9, 12, 13, 23–25]. The more recent definitive work of Groppo et al. with in situ Cr K-edge XANES/EXAFS demonstrated with direct monitoring of the surface chromia species on silica that surface Cr^{+2} sites are present after CO reduction. These studies, however, are somewhat complicated by the presence of 40 % Cr_2O_3 nanoparticles in their supported CrO_x/SiO_2 catalyst [15]. The UV–Vis band at 833 nm was assigned to Cr^{+2}, but is quite close to the UV–Vis band of bulk Cr_2O_3 at 810 nm. Most researchers agree that multiple surface Cr^{+2} sites are present on silica after activation with CO at elevated temperatures (see Table 1). The molecular structure of the Cr^{+2} site(s) still needs to be addressed and is complicated by possible presence of two distinct surface Cr^{+2} sites from the initial isolated dioxo and mono-oxo surface chromates on silica.

5.2 Activation of CrO_x with H_2

Activation studies involving H_2 are relatively rare and none of the studies applied spectroscopic methods to directly monitor the nature of the reduced surface CrO_x sites on silica. All the reported H_2 activation studies employed H_2-TPR, with or without TGA, to investigate the reduction features of the supported CrO_x sites on silica. Hogan found with TGA that oxygen consumption from the supported CrO_x/SiO_2 was greater with CO than H_2 [11]. This was also confirmed by the final colors of the activated CrO_x/SiO_2 catalysts that showed a gray-green color with H_2 reduction and a blue color with CO reduction that are characteristic of Cr^{+3} and Cr^{+2}, respectively.

Gaspar et al. also applied H_2-TPR spectroscopy to investigate the reduction of supported CrO_x/SiO_2 catalysts [26]. The H_2-TPR reduction peak(s) were found to depend on the Cr loading (~479 °C for 0.5 % Cr, ~496 °C for ~1 % Cr, and at ~376 °C and ~470 °C for ~3 % Cr). The H_2-TPR peaks at the higher temperatures were ascribed to reduction of surface $Cr^{+6} \rightarrow Cr^{+3}$ and the peak at 649 K for the higher Cr loading was assigned to reduction of large $Cr^{+6}O_3$ particles → Cr^{+3} that formed because the amount of hydroxyls was not sufficient to stabilize all the chromium on the silica surface [26]. The CrO_3 particles, however, would have thermally decomposed to Cr_2O_3 particles during the 500 °C calcination and would not be present. Although UV–Vis spectra were collected before H_2-TPR, the broad nature of the UV–Vis bands prevented clear structural assignments of the surface chromia species on silica as already discussed above. After H_2-TPR, all the reduced supported CrO_x/SiO_2 catalysts possessed UV–Vis bands at 272, 355, 467 and 610 nm that were assigned to

Cr^{+3}. In agreement with Hogan, the final oxidation state resulting from H_2 reduction was concluded to be Cr^{+3} [11].

5.3 Activation of CrO_x with C_2H_4

Activation studies with C_2H_4 are also limited because of complications associated with the presence of multiple hydrocarbons and possibly the H_2O reaction product that can interact with the surface CrO_x sites on silica [11]. A recent detailed in situ XANES/EXAFS study by Groppo et al. [15] monitored ethylene activation of supported CrO_x/SiO_2 catalysts and found that the catalyst exhibits features different than the CO-activated catalyst, which exhibits an oxidation state of Cr^{+2}. The C_2H_4-reduced CrO_x/SiO_2 catalyst yields a XANES spectrum with a higher intensity of the white line, reflecting an increased average Cr coordination, and the Cr^{+2} fingerprint is not present, which suggests that all surface isolated CrO_x sites are involved. Additionally, as seen in the corresponding EXAFS, these surface sites are not Cr^{+2} dimers because there is no signal for Cr–Cr in the second coordination shell [15]. The fraction of surface Cr sites interacting with ethylene has previously been proposed to vary from 10 to 55 % depending on the probe method [27–29], but these claims were based on indirect measurements and are not supported by this new direct XAS measurement indicating that all the dispersed Cr sites are involved [15]. The difference in the states of the surface CrO_x sites on silica upon CO reduction and C_2H_4 reduction were further demonstrated by adsorbing ethylene on a catalyst that had been pre-reduced with CO. Adsorption of ethylene on the Cr^{+2} sites increased the white line intensity (slight increase in coordination of Cr^{+2}) and completely removed the Cr^{+2} finger print in the pre-edge region. These results clearly demonstrate that the surface Cr^{+2} sites formed with CO reduction are not involved in ethylene polymerization reaction at room temperature (and low ethylene pressure) and that all the reduced surface Cr^{+2} sites are oxidized upon exposure to ethylene. This work nicely demonstrates that reduction in different environments leads to different activated surface CrO_x states on SiO_2 and that it is important not to confuse results from one reducing agent with another.

5.4 Activation of Well-Defined Catalysts With C_2H_4

Recent studies by Copéret et al. have examined the polymerization activities of well-defined model catalysts, dinuclear Cr^{+2} and Cr^{+3} model compounds and mononuclear Cr^{+3} model compounds, anchored on SiO_2 [30, 31]. The grafted dinuclear model $(\equiv SiO)_4Cr^{+2}{}_2$ and $(\equiv SiO)_6Cr^{+3}{}_2$ compounds were characterized by in situ IR, Cr K-edge XAS, and EPR spectroscopy before and after ethylene polymerization. The IR spectrum of $(\equiv SiO)_4Cr^{+2}{}_2$ only contained new silanol vibrations and no C–H stretches before exposure to ethylene. X-ray crystallographic analysis of a molecular model closely related to $(\equiv SiO)_6Cr_2$ revealed two five-coordinate Cr^{+3} centers (distorted trigonal bipyramidal and square-pyramidal geometry). The IR spectrum of $(\equiv SiO)_6Cr^{+3}{}_2$ after exposure to ethylene possessed C–H stretches and a white film formed on the pellet indicating polyethylene formation. The XANES spectrum of $(\equiv SiO)_4Cr^{+2}{}_2$ did not undergo any changes during the synthesis procedure. The initial ethylene polymerization activity of $(\equiv SiO)_6Cr^{+3}{}_2$ was an order of magnitude higher than $(\equiv SiO)_4Cr^{+2}{}_2$ suggesting that Cr^{+3} is the catalytic active site for this reaction. The EPR spectrum of $(\equiv SiO)_4Cr^{+2}{}_2$ taken before exposure to ethylene showed a weak signal for Cr^{+3}, suggesting that the minor amount of Cr^{+3} is most probably responsible for the polymerization activity [30]. Similar high initial polyethylene polymerization activity was also found for the mononuclear $(\equiv SiO)_3Cr^{+3}$ model compound consistent with the role of Cr^{+3} sites for ethylene polymerization [28]. Furthermore, the same initial ethylene polymerization rate was also obtained with a traditional CO-activated supported CrO_x/SiO_2 catalyst consistent with the role of surface Cr^{+3} sites for ethylene polymerization [32]. These new findings further support the role of Cr^{+3} sites on silica as the active sites, but may not necessarily be identical to the traditional catalyst.

6 Structure–Activity Relationship for Supported CrO_x/SiO_2 Catalysts

Developing fundamental structure–activity relationships requires knowing the molecular structure of the catalytic active site(s). This is rather complicated for traditional supported CrO_x/SiO_2 catalysts since two distinctive isolated surface chromia sites are initially present in the oxidized catalyst: dioxo $(O=)_2CrO_2$ and mono-oxo $O=CrO_4$. Thus, developing structure–activity relations requires knowing the concentrations of the two surface chromia sites and their specific activities, which is quite challenging. Consequently, the reported studies to date have assumed that only one surface CrO_x site is present on SiO_2 and only focused on the average oxidation state, which appears to primarily be surface Cr^{+3} during ethylene polymerization from the above review of activation of supported CrO_x sites by ethylene. The establishment of fundamental molecular structure–activity relationships for ethylene polymerization on each surface chromia site present in supported CrO_x/SiO_2 catalysts still awaits resolution with future studies.

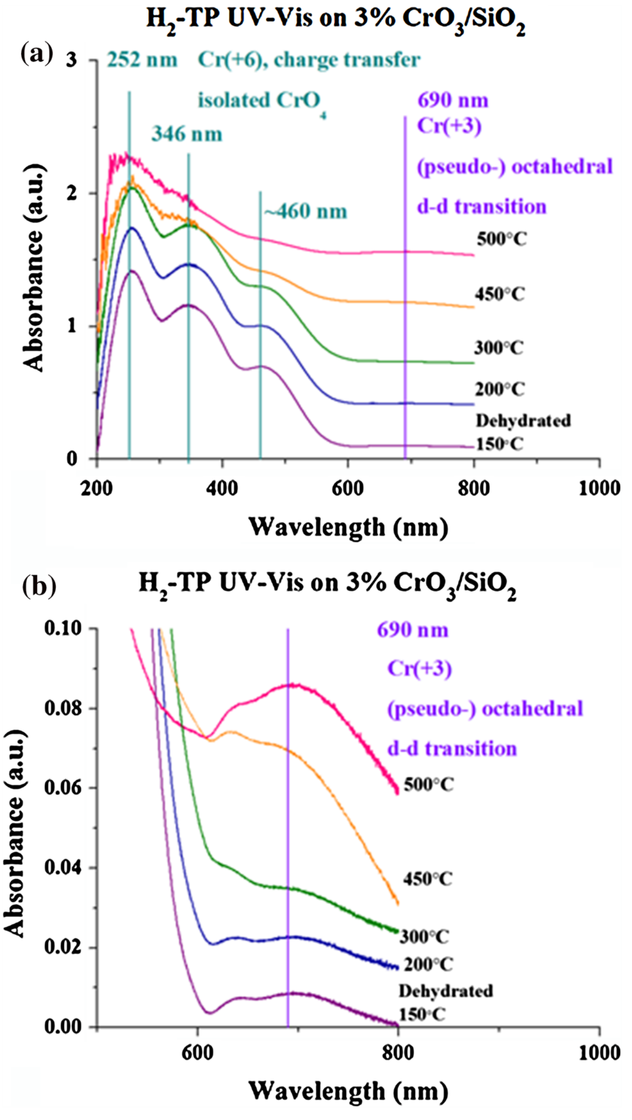

Fig. 4 In situ H_2 TP–UV–vis DRS of 3 % CrO_3/SiO_2 (a) full spectrum and (b) zoomed in to see the Cr^{+3} band. The 3 % CrO_3/SiO_2 catalyst was heated to 500 °C at 10 °C/min in 10 % O_2/Ar, held at 500 °C for 1 h, and cooled to 150 °C. It was then flushed for 30 min in Ar. Then the temperature was ramped to 500 °C in 4.8 % H_2. Spectra were taken every 50 °C

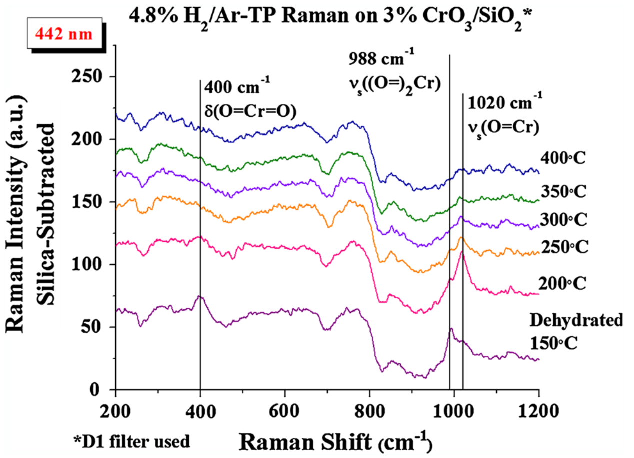

Fig. 5 In situ TP–Raman spectroscopy of 3 % CrO_3/SiO_2 in 4.8 % H_2/Ar after subtracting the silica support spectrum. The 3 % CrO_3/SiO_2 catalyst was heated to 500 °C at 10 °C/min in 10 % O_2/Ar, held at 500 °C for 1 h, and cooled to 150 °C. It was then flushed for 30 min in Ar. Then the temperature was ramped to 500 °C in 4.8 % H_2/Ar. Spectra were taken every 50 °C with the 442 nm laser and a D1 filter

New insights about the structure–activity relationships of supported CrO_x/SiO_2 catalysts are provided below from H_2-TPR studies. Although H_2 reduction kinetics are not ethylene polymerization kinetics, the reduction of the surface chromia sites on silica is the initial step in activating surface chromia for ethylene polymerization.

The electronic structures of the surface CrO_x sites on silica during H_2-TPR were monitored with in situ UV–Vis DRS and the spectra are presented in Fig. 4. The UV–Vis spectra revealed that the reduced catalyst has a Cr^{+3} oxidation state and is in an octahedral coordination. The initial dehydrated supported CrO_x/SiO_2 catalyst possesses LMCT transfer bands at 252, 346 and 460 nm that are characteristic of surface $Cr^{+6}O_x$ sites on silica [14]. During H_2-TPR, the UV–Vis $Cr^{+6}O_x$ LMCT bands decrease with increasing temperature and a new UV–Vis d–d band monotonically increases at ~690 nm that corresponds to surface $Cr^{+3}O_6$ sites [33]. The UV–Vis d–d transitions for $Cr^{+3}O_6$ sites should also be accompanied by additional bands at ~288 and 383 nm, but incomplete reduction of the $Cr^{+6}O_x$ LMCT bands in the same region prevents detection of these additional weak d–d bands. The intense green color of the H_2 reduced supported CrO_x/SiO_2 is consistent with the dominance of surface Cr^{+3} sites on silica. Thus, both the initial fully oxidized surface dioxo $(O=)_2CrO_2$ and mono-oxo $O=CrO_4$ sites on the SiO_2 support appear to reduce to surface $Cr^{+3}O_6$ sites during H_2-TPR.

The in situ H_2-TP Raman spectra supported for the supported 3 % CrO_x/SiO_2 catalyst are presented in Fig. 5. The Raman spectrum of the initial dehydrated CrO_x/SiO_2 catalyst at 150 °C exhibits bands at ~988 and ~1020 cm^{-1}, for the dioxo and mono-oxo CrO_x species, respectively, and at ~400 cm^{-1} from the CrO_x bending vibrations. In flowing hydrogen at 200 °C, the Raman band at ~988 cm^{-1} from the surface dioxo species rapidly diminishes relative to that from the band at 1020 cm^{-1} from the surface mono-oxo species. The Raman band at ~1020 cm^{-1} of the surface mono-oxo species continuously decreases with increasing temperature from 200 to 400 °C and is almost completely reduced at 400 °C.

The relative concentrations of the surface dioxo $(O=)_2CrO_2$ and mono-oxo $O=CrO_4$ sites on silica and their H_2 reduction kinetics were chemically probed with H_2-TPR as shown in Fig. 6. As shown above in Fig. 5 for the H_2

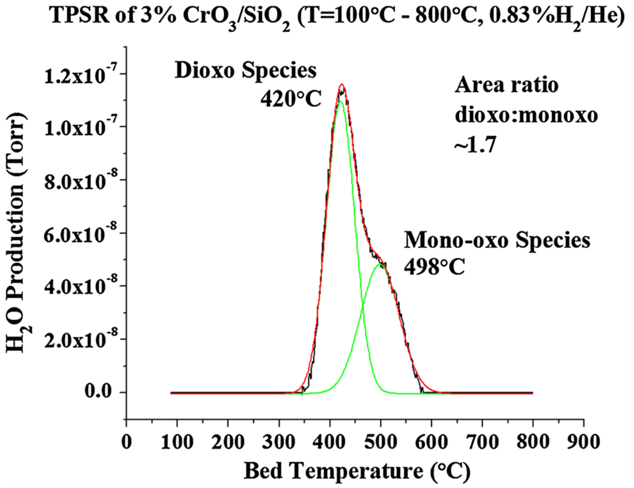

Fig. 6 H_2-TPSR of 3 wt% CrO_3/SiO_2. The 3 % CrO_3/SiO_2 catalyst was heated to 500 °C at 10 °C/min in 10 % O_2/Ar, held at 500 °C for 1 h, and cooled to 150 °C. It was then flushed with UHP He. Then the temperature was ramped to 800 °C in 0.83 % H_2/He. H_2O production was monitored

TP-Raman spectra, the surface dioxo species reduce prior to the surface mono-oxo chromia species on silica. Deconvolution of the H_2-TPR spectrum of the supported 3 % CrO_x/SiO_2 catalyst found that the surface chromia phase consists of ~2/3 surface dioxo sites and ~1/3 surface mono-oxo sites (exact dioxo:mono-oxo ratio ~1.7). These findings are in agreement with the DFT calculations by Handzlik et al. that predicted that dioxo surface $(O=)_2CrO_2$ sites should be much more stable than mono-oxo surface $O=CrO_4$ sites on the SiO_2 support [19]. The H_2 reduction kinetics for the surface dioxo and mono-oxo chromia sites on silica are also provided from the peak temperatures (Tp) during the H_2-TPR experiments by application of the Redhead equation for first-order reactions [34, 35]. The Arrhenius rate constants for H_2-TPR reduction of the surface dioxo and mono-oxo chromia sites are 0.30/s and 8.2×10^{-3}/s, respectively, at a reference temperature of 500°C. Thus, the surface dioxo $(O=)_2CrO_2$ sites on silica represent about 2/3 of the supported chromia phase and their H_2 reduction kinetics are ~37 times faster than that for the surface mono-oxo $O=CrO_4$ sites on silica at 500 °C and much higher at lower temperatures. The reduction kinetics indicate the more facile activation of surface dioxo $(O=)_2CrO_2$ than surface mono-oxo $O=CrO_4$ sites on silica. This is the first time that molecular structure–activity relationships have been established for supported CrO_3/SiO_2 catalysts. Future studies will establish the molecular structure–activity relationships for ethylene polymerization by the dioxo and mono-oxo chromia sites on SiO_2 catalysts.

7 Conclusions

The nature of the surface CrO_x sites strongly depends on the environment to which the supported CrO_x/SiO_2 catalysts are exposed. Under ambient conditions, hydrated surface chromia species are present (CrO_4, Cr_2O_7, Cr_3O_{10} and Cr_4O_{13}) and the extent of oligomerization increases with decreasing surface pH values at point of zero charge. Under dehydrated and oxidizing conditions, the surface chromia sites are present as isolated surface dioxo $(O=)_2CrO_2$ and mono-oxo $O=CrO_4$ with a ratio of ~2/1 on silica that is independent of coverage below the maximum dispersion limit. Crystalline Cr_2O_3 nanoparticles are also present above the maximum dispersion limit, which depends on the Cr precursor, solvent and surface properties of the SiO_2 support. Many of the early studies applied UV–Vis spectroscopy to determine the nature of the surface CrO_x sites on silica, but it turns out that the broad and overlapping UV–Vis bands prevented clear cut structural assignments. The supported CrO_x/SiO_2 catalysts are activated for ethylene polymerization by exposure to reducing environments. Activation with CO leads to Cr^{+2} sites, but activation with H_2 and C_2H_4 results in Cr^{+3} sites. For reduction by H_2, the initial surface dioxo site is ~37 times more easily reduced than the initial surface mono-oxo site reflecting the greater ease of activation of the surface dioxo site than mono-oxo site in reducing environments. Similar fundamental molecular structure–activity relationships still need to be developed for ethylene polymerization by supported CrO_x/SiO_2 sites.

References

1. Hogan JP (1983) In: Leach BE (ed) Applied industrial catalysis, vol 1. Academic Press, New York, pp 149–153
2. Groppo E, Lamberti C, Bordiga S, Spoto G, Zecchina A (2005) Chem Rev 105:115
3. McDaniel MP (2010) In: Gates B, Knoezinger H, Jentoft F (eds) Advances in catalysis, vol 53. Elsevier, Waltham, pp 128–133
4. J.P. Hogan. Polymers and Production Thereof, US Patent 2,825,721 (March 4, 1958)
5. Hardcastle F, Wachs IE (1988) J Mol Catal 46:173
6. Vuurman MA, Wachs IE, Stufkens DJ, Oskam A (1993) J Mol Catal 80:209
7. Michel G, Cahay R (1986) Raman Spectrosc 17:79
8. Deo G, Wachs IE (1991) J Phys Chem 95:5889
9. Weckhuysen BM, Schoonheydt RA, Jehng J, Wachs IE, Cho SJ, Ryoo R, Kljlstra S, Poels E (1995) J Chem Soc Faraday Trans 91:3245
10. Zecchina A, Garrone E, Ghiotti G, Morterra C, Borello E (1975) J Phys Chem 79:966

11. Hogan JP (1970) J Polym Phys A-1 8:2637
12. Fubini B, Ghiotti G, Stradella L, Garrone E, Morterra C (1980) J Cat 66:200
13. Weckhuysen BM, De Ridder LM, Schoonheydt RA (1993) J Phys Chem 97:4756
14. Lee EL, Wachs IE (2007) J Phys Chem C 111:14410
15. Groppo E, Damin A, Bonino F, Zecchina A, Bordiga S, Lamberti C (2005) Chem Mater 17:2019
16. Groppo E, Prestipino C, Cesano F, Bonino F, Bordiga S, Lamberti C, Thüne PC, Niemantsverdriet JW, Zecchina A (2005) J Cat 230:98
17. Dines TJ, Inglis S (2003) Phys Chem Chem Phys 5:1320
18. Lee EL, Wachs IE (2008) J Phys Chem C 112:6487
19. Handzlik J, Grybos R, Tielens F (2013) J Phys Chem C 117:8138
20. J.P. Hogan. Method of treating chromium oxide catalyst and polymerization therewith, US Patent 3,362,946 (January 9, 1968)
21. Przhevalskaya LK, Shvets VA, Kazansky VB (1975) J Cat 39:363
22. Zecchina A, Garrone E, Ghiotti G, Coluccia S (1975) J Phys Chem 79:972
23. Rebenstorf B, Larsson R (1981) Z Anorg Allg Chem 478:119
24. Rebenstorf B, Larsson R (1981) J Mol Cat 11:247
25. Rebenstorf B, Sheng TC (1991) Langmuir 7:2160
26. Gaspar AB, Martins RL, Schmal M, Dieguez LC (2001) J Mol Cat A 169:105
27. McDaniel MP (1985) Adv Catal 33:47
28. Ghiotti G, Garrone E, Zecchina A (1988) J Mol Cat 46:61
29. Groppo E, Lamberti C, Cesano F, Zecchina A (2006) Phys Chem Chem Phys 8:2453
30. Conley MP, Delley MF, Siddiqi G, Lapadula G, Norsic S, Monteil V, Safonova OV, Copéret C (2014) Angew Chem Int Ed 53:1872
31. Delley MF, Núñez-Zarur F, Conley MP, Comas-Vives A, Siddiqi G, Norsic S, Monteil V, Safonova OV, Copéret C (2014) PNAS 111:11624
32. Delley MF, Conley MP, Copéret C (2014) Catal Lett 144:805
33. Weckhuysen BM, Wachs IE, Schoonheydt RA (1993) Chem Rev 96:3327
34. Redhead PA (1962) Vacuum 12:203
35. Lee EL, Wachs IE (2008) J Cat 258:103